BMC Research Notes

RESEARCH NOTE Open Access

Synthesis, physicochemical properties and antimicrobial activity of a di-aminopropionic acid hydrogen tri-iodide coordination compound

Seitzhan Turganbay[1,2*], Sabina Kenesheva[1,3*], Ardak Jumagaziyeva[1], Alexandr Ilin[1], Dana Askarova[1], Amir Azembayev[1] and Assel Kurmanaliyeva[1]

Abstract

Objective The objective of this study is to synthesize and comprehensively characterize a novel iodine-containing coordination compound, di-aminopropionic acid hydrogen tri-iodide. This involves determining its structural, physicochemical, and thermal properties, as well as evaluating its antimicrobial activity against a range of bacterial strains, including multidrug-resistant pathogens. The aim is to explore the potential of this compound as a candidate for developing new antibacterial agents to address the challenge of antibiotic resistance.

Results An original iodine-containing semiorganic coordination compound was synthesized and characterized. The physicochemical properties were studied via diffraction, FTIR spectroscopy and thermogravimetric/differential scanning calorimetry (TG/DSC). In vitro antimicrobial activity evaluation was performed using two-fold serial dilution method. The obtained results demonstrated efficiency against both gram-positive (*Staphylococcus aureus*) and gram-negative (*Escherichia coli*, *Pseudomonas aeruginosa*, *Acinetobacter baumannii*) bacteria including MDR strains that cause infectious disease. The results of the antibacterial evaluation revealed that the new iodine coordination compound – di-aminopropionic acid hydrogen tri-iodide possesses high bactericidal properties and exhibits better antimicrobial activity against both susceptible and multidrug-resistant strains than does Lugol solution and ampicillin sodium, which are used as reference drugs.

Keywords Alanine, Coordination compound, Iodine, Antimicrobial activity, multidrug resistance

*Correspondence:
Seitzhan Turganbay
turganbay.s@gmail.com
Sabina Kenesheva
silentium_n@bk.ru
[1]Laboratory of New Substances and Materials, JSC Scientific Center for Anti-Infectious Drugs, Almaty 050060, Kazakhstan
[2]"One Belt One Road" Petroleum Engineering Institute, Kazakh-British Technical University, Almaty 050000, Kazakhstan
[3]Faculty of Biology and Biotechnology, Al-Farabi Kazakh National University, Almaty 050040, Kazakhstan

Introduction

Nowadays, the reduction in the effectiveness of antibiotics against widespread bacterial infections constitutes a major threat to global health. The latest report from the 2022 Global Antimicrobial Resistance and Use Surveillance System (GLASS) highlights rising resistance rates among common bacterial pathogens. This increase in resistance may necessitate the greater use of last-resort drugs, such as carbapenems, which are now also encountering resistance in multiple regions. As the effectiveness of these last-resort drugs becomes compromised, the risk of untreatable infections rises [1, 2].

Iodine has been widely used as a disinfectant and antiseptic for many years due to its effectiveness as an antimicrobial agent. Its resistance to eliciting bacterial resistance may be attributed to its broad mechanism of action and extensive history of used. Among halogens, iodine is the least reactive element. Additionally, it is compatible with biological systems and plays a significant role in the production of thyroid hormones. Notably, iodine consistently demonstrates effectiveness against both gram-positive and gram-negative bacteria, including resistant strains, as well as fungi and protozoa [3– 5].

Furthermore, iodine has shown activity against a wide range enveloped and nonenveloped viruses [6, 7], as well as certain bacterial spores with extended exposure times. Studies have revealed that iodine-containing complexes, such as PVP-I, are effective against established bacterial and fungal biofilms in both laboratory and clinical experiments [8–14]. Laboratory findings further suggest that iodine not only exhibits broad-spectrum antibacterial effects but also mitigates inflammation triggered by pathogens and the host immune response [15].

The antimicrobial properties of iodine stem from its ability to disrupt critical bacterial cellular processes and structures. It oxidizes nucleotides, as well as fatty and amino acids, in bacterial cell membranes. Additionally, iodine disrupts bacterial metabolic processes by targeting cytosolic enzymes involved in the electron transport chain [16, 17].

Iodine-containing complexes are characterized by pronounced antimicrobial activity against gram-positive and gram-negative bacterial strains, including multidrug resistant forms. Moreover, current literature does not report confirmed cases of bacterial resistance to iodine-containing complexes [18–20]. Additionally, studies by other researchers have demonstrated the capacity of iodine-containing complexes to alter antibiotic susceptibility in multidrug-resistant microbial strains [21, 22]. Our previous research demonstrated that organic compounds derived from amino acids in iodine-containing complexes can modulate the impact of iodine on pathogens. When subjected to this treatment, *E. coli* ATCC BAA-196 and *S. aureus* ATCC BAA-39 showed a significant increase in the activity of heavy metal efflux pumps, suggesting a potential disruption of cell wall structure organization and increased permeability of the cellular membrane. Moreover, there was a notable effect on the genes regulating the oxidation–reduction balance in both bacteria, indicating the presence of oxidative stress [23].

The purpose of this research was to build upon previous studies and investigate the physical and chemical properties of this substance using various analytical techniques, including X-ray diffraction, UV–visible spectrophotometry, IR spectroscopy, thermogravimetric analysis (TGA), and energy-dispersive X-ray spectroscopy (EDX). These methods provide a more comprehensive understanding of the compounds' thermal stability, functional groups, and elemental composition of the compounds. Furthermore, we compared the antimicrobial activity of diaminopropionic acid hydrogen triiodide to that of Lugol's solution against susceptible and multidrug-resistant test strains. Given their potent antimicrobial effects, these complexes show potential for the development of new antibacterial medications targeting multidrug-resistant bacteria.

Materials and methods

Reagents and materials

All the reagents used in this study were obtained from commercial sources. Potassium iodide, iodine, L-alanine (≥ 99%) were obtained from Sigma–Aldrich (St. Louis, MO, USA), Nutrient agar, tryptic soy agar, and Muller-Hinton broth were purchased from Himedia (India). Ampicillin sodium salt was sourced from Merck (Germany). Sodium chloride (>99%) was obtained from Mikhailovsky Chemical reagents Plant (Russia), and ethanol (96%) was procured from Talgar Spirt' (Kazakhstan).

Test strains and growth conditions

The microbial test strains used in this study were obtained from the American Type Culture Collection (ATCC, Rockville, MD, USA) and included both susceptible and multidrug-resistant (MDR) bacteria strains. The most common gram-positive bacteria were the susceptible strains *Staphylococcus aureus* (6538-P) and MRSA (BAA-33591). The gram-negative bacteria included the susceptible strains *Escherichia coli* (8739) and *Pseudomonas aeruginosa* (9027), the MDR strain *Escherichia coli* (BAA-2523), *Acinetobacter baumannii* ATCC BAA-1790, and the clinical MDR isolate *Pseudomonas aeruginosa* TA2.

Stock cultures were stored at −80 °C under low-temperature conditions. Before the experimentation, the test strains were cultivated and passaged twice on Tryptic Soy Agar and Nutrient Agar, as recommended by the ATCC.

The cells were incubated at 37 °C for 18–24 h (Binder, Germany).

X-ray diffractions analysis

The samples were analyzed using an Auto-Refractometer CAD4 Enraf-Nonius (Rotterdam, Netherlands) equipped with the pre-installed CAD4 version 5 software. Radiation source: Cu Kα radiation (wavelength 1.5418 Å), providing high-intensity X-rays suitable for crystalline material analysis. Scanning speed: 5°/min, 2θ range: 5° to 60°.

UV–vis spectroscopy

UV–vis spectra of the samples were collected using a LAMBDA-35 UV–vis spectrophotometer (PerkinElmer, USA). The samples were dissolved in a water solution (1 mg/mL), and the solvent was used as a reference. The scanning range was 190–1100 nm.

Fourier transformed infrared (FTIR) spectroscopy

The infrared spectra of the investigated samples were recorded using a NICOLET 6700 Fourier-transform infrared (FTIR) spectrometer from Thermo Scientific. The instrument was equipped with a SMART PERFORMER attachment utilizing a ZnSe crystal by the internal reflection. A sample amount between 0.05 and 0.1 g was finely ground in a porcelain mortar and then placed on the ZnSe crystal of the SMART PERFORMER attachment. The absorption spectrum in the infrared region was recorded over the wavelength range from 650 to 4000 cm^{-1} at room temperature.

Thermal analysis (TG/DSC)

Thermal analysis performed using a synchronous thermal analyzer STA 449 F1 Jupiter (Netzsch), which allows simultaneous measurement of mass changes (thermogravimetry) and heat flow (differential scanning calorimetry). Samples weighing 1–5 mg were heated in a temperature range from 28 °C to 600 °C in closed corundum crucibles with a volume of 85 µL at a heating rate of 10 °C/min in a dry nitrogen atmosphere (gas flow rate 40 cm^3/min).

Differential curves of the sample's heat capacity changes (DSC) were recorded on the thermograms. Melting temperatures of the substances were determined using Netzsch-Proteus software by locating the intersection points of tangents drawn at the start of the endothermic peak on the DSC curve. This method allowed for precise identification of the onset temperature of the peak, which was used to determine the sample's melting temperature.

Elemental analysis

Elemental analysis of the [2Ala·HI_3] coordination compound was performed using energy-dispersive X-ray spectroscopy (EDS) integrated with a scanning electron microscope (SEM), model Quanta 3D 200i (FEI, Netherlands). This method determines the chemical composition of a material by analysing the X-ray emissions generated when the sample is irradiated with an electron beam.

Synthesis of the [2Ala·HI_3] coordination compound

To synthesize the [2Ala·HI_3] coordination compound, 3.19 g (0.036 mol) of alanine was dissolved in 20 mL of purified water in a 50 mL beaker. The mixture was heated in a 40 °C water bath and stirred with a glass rod until the amino acid fully dissolved. The molar ratios of alanine, KI, and iodine were maintained at 2:3:1, with an excess of potassium iodide and iodine required for the complete reaction of alanine.

Separately, 8.96 g (0.054 mol) of potassium iodide and 4.54 g (0.018 mol) of iodine were finely powdered using an agate mortar and pestle and dissolved in 20 mL of purified at room temperature (RT). The resulting potassium triiodide solution was added to the alanine solution in a 50 mL flask with a stopper. The reaction mixture was sealed and stirred at RT for 5 min, followed by 48 h of storage in the dark at RT to allow the system to reach equilibrium. Afterward, the mixture was heated in 50 °C water bath for 10 min and filtered under vacuum using a Schott filter into a crystallizer. The crystallizer was placed in a dark glass desiccator containing anhydrous calcium chloride as a desiccant to evaporate most of the water. The resulting crystals were collected under vacuum using a Schott filter, washed twice with ethanol cooled to 0 °C, and further dried on an ashless black tape filter. The crystals were weighed, transferred to a flask with a glass stopper, and stored in a refrigerator. The final yield was 8.50 g (85%) of single crystals. The synthesis process for the [2Ala·HI_3] coordination compound is illustrated in Fig. 1.

In vitro antimicrobial activity assay

The antimicrobial activity assay was performed using a twofold serial broth microdilution method based on the Clinical and Laboratory Standards Institute guidelines, with some modifications [24–26]. The experiments were conducted in sterile 96-well polystyrene plates (BIOLOGIX, Jinan, Shandong, China).

Serial twofold dilution preparation

Each well of the 96-well plate was filled with 100 µL of 0.9% saline. Subsequently, 100 µL of the iodine-containing compound solution was added to the first well in the raw (A1). Serial twofold dilutions were then carried out: 100 µL of the saline and iodine-containing

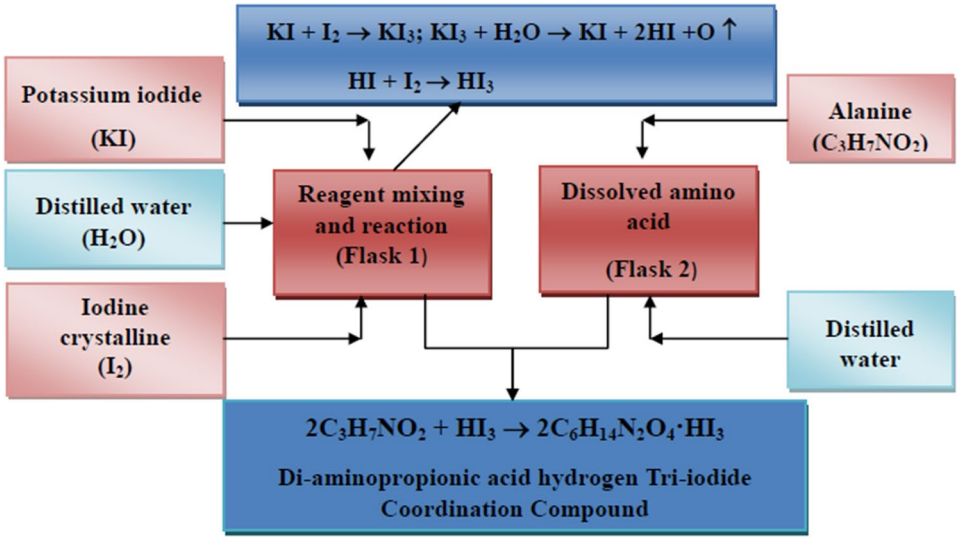

Fig. 1 Chemical flow chart of the synthesis of the [2Ala·HI_3] coordination compound

compound solution from the first well (A1) was mixed and transferred into the second well (A2). This process was repeated, transferring 100 µL of the twice-diluted solution from well (A2) into well A3, and so on, until the required number of dilutions was achieved.

The iodine-containing compounds were dissolved in 0.9% saline to an initial concentration of 1000 µg/mL (with an I_2 concentration of 125.1 µg/mL). Two controls were included in this study. Lugol's solution as the reference iodine-containing agent and the broad-spectrum antibiotic ampicillin as a positive control for antimicrobial activity.

The antimicrobial activity of ampicillin was assessed using the same twofold serial microdilution method without modifications. The initial concentration of ampicillin sodium was 16 000 µg/mL. All experiments were conducted in triplicate.

Cell suspension preparation and inoculation

Bacterial cell suspensions were prepared by harvesting 1824 h incubated test strain colonies with a sterile inoculating loop and transferring them to a test tube containing sterile saline. The bacterial suspension was homogenized, and its cell density was adjusted to 0.5 McFarland Units (DEN-1, Latvia), corresponding to a concentration of 1.5×10^8 CFU/mL.

The stock cell inoculum was diluted 100-fold with sterile saline to produce a working suspension with a final concentration of ~1.5×10^6 CFU/mL. A 10 µL aliquot of the bacterial suspension was added to each well in the plate row. Following 30 min of incubation at 37 °C, 10 µL suspensions from each well were streak onto nutrient agar or tryptic soy agar plates.

Table 1 Physicochemical properties of the synthesized [2Ala·HI_3] coordination compound

No	Name of indicators	Results
1	Empirical formula	$C_6H_{15}N_2O_4\cdot I_3$ or (2Ala·HI_3)
2	Molecular Weight, g/mol	559.7
3	pH	3.62
4	Solubility in water, g/100 ml	20 g (at 25 °C)
5	Melting temperature (°C)	125.6
6	Colour	Dark brown
7	Iodine content, (%)	67.89
10	Final mass, g	8.50
11	Yield (%)	85

Determination of antimicrobial activity

The results of ampicillin's antimicrobial activity were visually assessed by observing turbidity in the broth media. The minimal bactericidal concentrations (MBCs) of the iodine-containing compounds were determined as the lowest concentrations that completely inhibited culture growth after 30 min of incubation. The minimal inhibitory concentrations (MICs) of ampicillin were identified as the lowest antibiotic concentrations that visibly inhibited bacterial growth in the wells.

Results and discussion

Physicochemical analysis of the [2Ala·HI3] coordination compound

The physicochemical properties, including colour, percentage yield, melting point, and decomposition temperature of the synthesized coordination compound, are summarized in Table 1. The [2Ala·HI3] complex dark brown in colour and demonstrated high solubility in water, but it was insoluble in most organic solvents such as benzene, cyclohexane, chloroform, and *o*-xylene. Following the OECD guidelines for chemical

testing (water solubility), the solubility of the [2Ala·HI_3] coordination compound was determined using the Flask method, which is suitable for substances with solubility values exceeding 0.01 g/L. The results of the analysis are detailed in Table 1.

The data demonstrated that the [2Ala·HI_3] complex exhibits unique solubility characteristics and a high iodine content (67.89%) highlights its potential as a potent iodine career, which could be significant for applications in antimicrobial agents or iodine supplementation therapies.

X-ray diffractions analysis of [2Ala·HI3] coordination compound

Single-crystal X-ray diffraction analysis was performed using an Auto-Refractometer CAD4 Enraf-Nonius (Rotterdam, Netherlands) equipped with pre-installed CAD4 version 5 software. The measurements were conducted at 200±1 K to preserve the integrity of the crystals and prevent thermal damage. The analysis was carried out on suitable light-red, plate-shaped crystals, which were carefully selected for their quality and compatibility with the method. Experimental conditions and key crystallographic parameters are summarized in Table 2.

The unit cell parameters, determined based on 25 reflections, confirmed a monoclinic crystal system. A search for structurally similar compounds in the Cambridge Structural Database of Organic Compounds (CCDC) verified the originality of this compound. According to the calculation results, the chemical formula of the obtained compound can be represented as $[C_6H_{15}N_2O_4]^{+1}I_3^{-1}$. Interatomic distances and bond angles in the crystal structure are presented in Tables S1 and S2.

The structural study of compound № 25 revealed that the molecule is a dimer composed of two alanine molecules connected by a hydrogen bond between the oxygen atoms of the carboxyl groups (Fig. 2). At the same time, in this hydrogen bond, the acceptor alternates between the oxygen atoms O6, which belong to the alanine molecules forming the dimer, and another one. In the dimer, both nitrogen atoms are quaternary, resulting in a dimer with a charge of +1, which is balanced by the I_3^{-1} polyanion.

In the three-dimensional molecular packing (Fig. S1), all three hydrogen atoms of the quaternary nitrogens participate in the formation of hydrogen bonds (Table S3). Specifically, the hydrogen bonds N4–H4A…O5 and N4–H4B…O6 align parallel to the plane (100), linking alanine dimers into a two-dimensional network (Fig. S2). Meanwhile, the hydrogen bonds N4–H4C…I1 and N4–H4C…I1 connect these layers into a three-dimensional structure via I_3^{-1} polyanions (Figs. S3 and S4).

Table 2 Basic crystallographic data $C_6H_{15}N_2O_4{\cdot}I_3$

Crystal Data	
Formula	$C_6H_{15}N_2O_4{\cdot}I_3$
Formula Weight	559.90
Crystal System; Space group	Monoclinic; $P2_1/c$
Lattice constants a, b, c [Å]	8.1057(16), 8.9853(18), 10.541(2)
alpha, beta, gamma [deg]	90, 100.29(3), 90
V [Å]^3; Z	755.4(3); 2
D(calc)[g/cm^3]; F (000)	2.462; 512
Mu (MoKα) [mm^{-1}]	6.205
Crystal Size [mm]	0.10×0.10×0.20
Data Collection	
Temperature (K); Radiation [Å]	200; MoKα; λ = 0.71073
θ_{min}; θ_{max} [Deg]	2.6, 30.0
Dataset	0: 11; 0: 12; -14: 14
Tot., Uniq. Data, R(int)	2338, 2195, 0.023
Observed data [I > 2.0 sigma(I)]	1737
Refinement	
Nref, Npar	2195, 102
R, wR^2, S	0.0351, 0.0859, 1.10
w = 1/[\s^2^(Fo^2^) +(0.0374P) ^2^+0.2440P] where P=(Fo^2^+2Fc^2^)/3	
Max. and Av. Shift/Error	0.00, 0.00
Min. and Max. Resd. Dens. [e/Å^3]	-1.03, 1.45

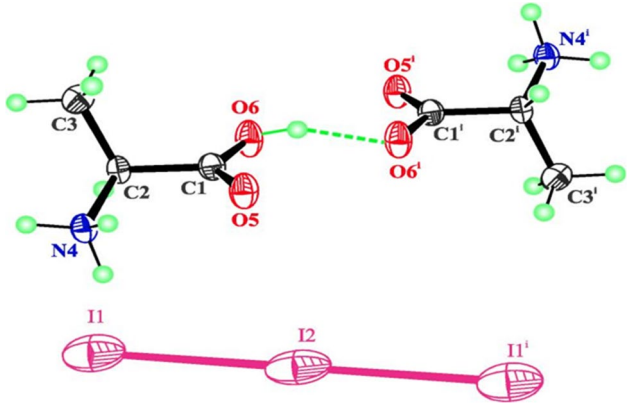

Fig. 2 Atomic model of the $C_6H_{15}N_2O_4{\cdot}I_3$ structure. Anisotropic thermal vibration ellipsoids are drawn at the 50% probability level

Electronic spectra of [2Ala·HI3]coordination compound

Spectral characteristics of the L-alanine ligand and coordination compound are presented in Fig. 3. The electronic absorption spectrum shows a weak broad peak near 275 nm corresponds to L-alanine in water and can be attributed to (π→π*) transition of (C=O) in the biguanide group. On the contrary, [2Ala·HI_3]coordination compound showed three major absorption bands at 223.34 (0.85 A), 285.08 (0.05 A), and 349,98 nm (0.03 A), respectively The bands at 223 nm and 285 nm are due to the presence in solution of molecular iodine complexes coordinated by the carboxy group of alanine and potassium ion and correspond to the charge transfer bands from the ligand to the iodine molecule.The bands of

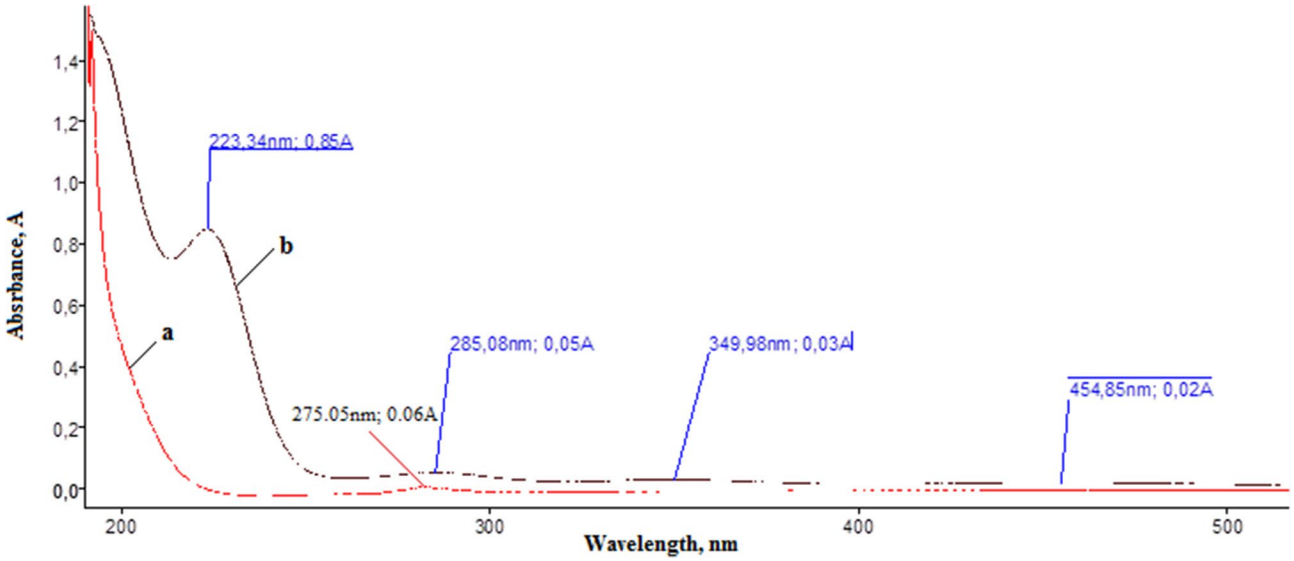

Fig. 3 UV spectrum of (**a**) alanine and (**b**) [2Ala·HI_3] coordination compound

349 nm and 454 nm are due to the existence in the solution of the tri-iodide complex coordinated by hydrogen atoms of the positively charged amino group and correspond to the transitions between free and occupied MO in tri-iodide. These results confirm that the coordination compound [2Ala·HI_3] consists of an iodine - L-alanine complex.

Infrared spectra of the [2Ala·HI3] coordinated compounds

The vibrational IR spectra of the synthesized [2Ala·HI_3] coordination compound, are shown in Fig. 4, provide insights into the molecular interactions and structural changes occurring during complexation [27, 28]. The analysis indicates that both the carboxyl and amino groups of the alanine molecules participate in the formation of the coordination complex.

A key observation is the shift of the band at 1352.2 cm^{-1} by 7 cm^{-1} to the long-wavelength region, along with the emergence of a new band at 1719.9 cm^{-1}. These features are attributed to the vibrations of oxygen-containing functional groups, specifically suggesting the formation of hydrogen bonds involving the carboxyl groups of alanine molecules.

The appearance of new bands at 1612.5 cm^{-1} and 1505.4 cm^{-1}, corresponding to the symmetric deformation vibrations of the quaternary amino group (-NH_3^+), suggests additional interactions. These bands indicate the establishment of hydrogen bonds between the positively charged quaternary protons of the amino group and the negatively charged polyiodide anions.

Further evidence supporting the interaction between the alanine molecule and the polyiodide anion is the shift of the band at 3076.6 cm^{-1} to 3060.2 cm^{-1} in the spectrum of the coordination complex. This shift of 16 cm^{-1} reflects the influence of hydrogen bonding and charge redistribution of the N-H stretching vibrations.

The IR spectra confirm the involvement of alanine's functional groups in the complexation process, primarily through hydrogen bonding interactions that stabilize the [2Ala·HI_3] coordination compound. These findings highlight the intricate role of hydrogen bonding in determining the molecular structure of the complex.

EDX spectra of the [2Ala·HI3] coordination compound

Energy-dispersive X-ray spectroscopy (EDX) was employed to identify the chemical elements presented in the [Ala·HI_3] coordination compound and estimate their relative abundances. The EDX analysis produces spectra with peaks corresponding to the consistent elements in the sample, as shown in Fig. 5. This method also enables elemental mapping and image analysis to assess the uniform distribution of elements in the sample.

The EDX results for the [Ala·HI_3] coordination compound indicate that the weight percentages of iodine, carbon, nitrogen, and oxygen were 66.83%, 4.68, 11.17, and 11.78, respectively. (Table 3). Hydrogen content was estimated indirectly from the difference between the total sample mass and the measured elemental masses. These results are consistent with the proposed empirical formula of the complex and confirm its structural integrity.

Furthermore, the uniformity of the elemental distribution across all analysed points supports the homogeneity of the sample. This homogeneity is essential for validating the reproducibility and consistency of the synthesis method. The high iodine content aligns with the coordination of iodine in the compound and highlights its potential applications in iodine-based therapeutic or antimicrobial formulations.

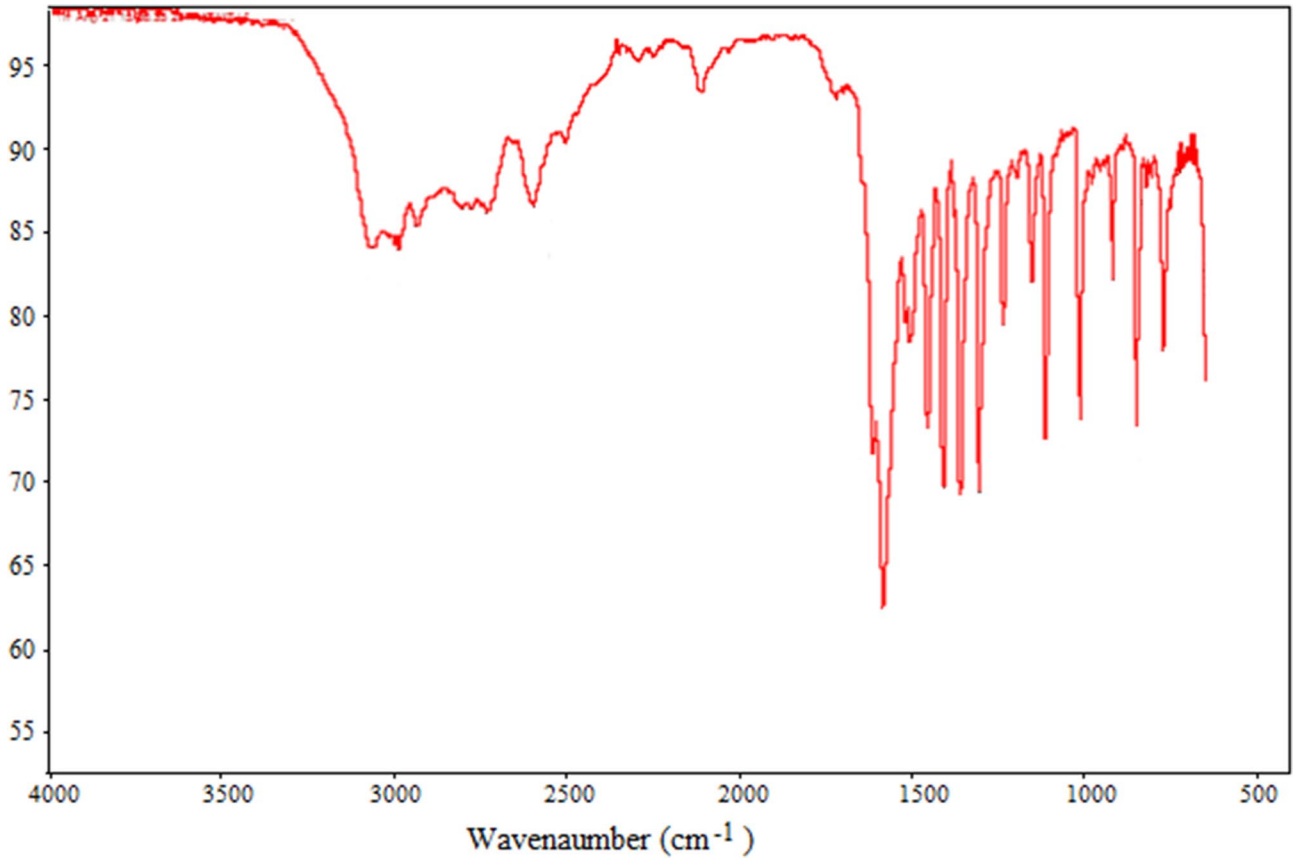

Fig. 4 Infrared spectra of the [Ala·HI_3]coordinated compounds

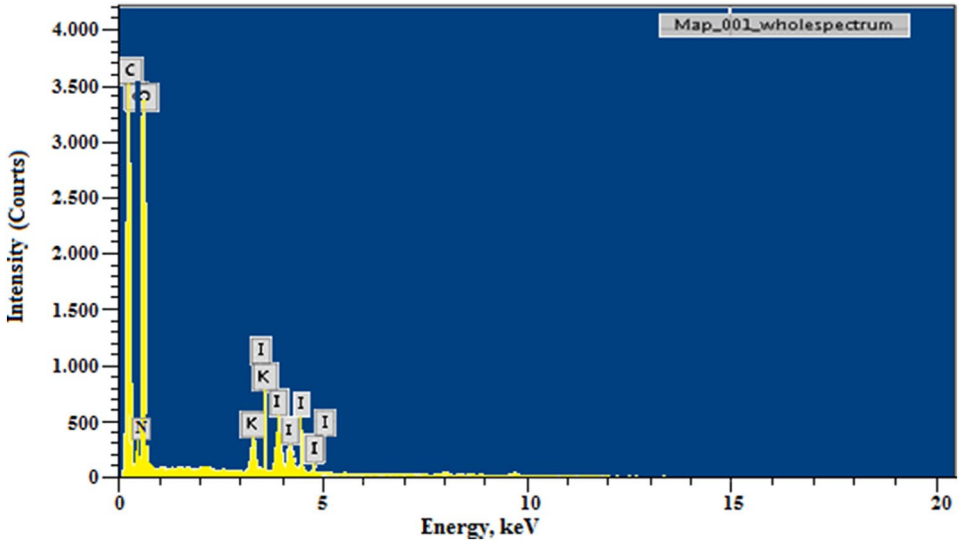

Fig. 5 EDX spectrum of the [2Ala·HI_3] coordination compound

Thermal analysis by TGA/DSC

The thermal behaviour of the [2Ala·HI_3] coordination compound was analysed using thermogravimetric analysis (TGA) and differential scanning calorimetry (DSC), as shown in Fig. 6. The melting point of the complex, identified as 125.6 °C on the DSC curve, aligns with the melting point measurement obtained using the Gallenkamp variable heating device (Table 4), confirming the consistency of the results.

Table 3 Energy dispersive X-ray (EDX) spectroscopy

Element	Weight% (theory)	Weight% (found)	Line type
C-Ka	12.68	11.78	K Series
N-Ka	5.00	4.68	K Series
O-Ka	11.43	11.17	K Series
I-La	68.02	66.83	L Series
H	2.68	-	-
Totals	99.81	94.46	-

*The hydrogen content was calculated based on the mass difference between the sample and the elements determined experimentally

The thermal decomposition of [2Ala·HI_3] proceeds through two distinct stages, as indicated in Fig. 6; Table 4: (1) Stage 1: 28–120 ºC, in the first stage, residual water molecules are eliminated in a single step, resulting in a 7.26% mass loss. The DSC curve shows a corresponding endothermic peak at approximately 40.85 ºC, consistent with the dehydration process. (2) Stage II: at temperatures above 125,6 °C, is associated with the thermal degradation of the [2Ala·HI_3] complex, resulting in a mass loss of 90,42%. After heating to 500 °C, the ash content was 2,32% of the initial weight.

According to literature data, the melting point of alanine is typically in the range of 295–300 °C [29]. These values are somewhat higher than the melting point of the [2Ala·HI_3] complex, which is 125,6 °C, indicating a change in thermodynamic properties caused by specific interactions within the complex.

The TGA/DSC analysis demonstrated a complete mass loss of 100%, confirming that the [2Ala·HI_3] complex is chemically pure and undergoes full thermal decomposition. This behaviour also underscores the thermostability of the compound under the experimental conditions.

Evaluation of biological activities

The antibacterial potential of the newly synthesized diaminopropionic acid hydrogen tri-iodide [2Ala·HI_3] coordination compound was evaluated against both gram-positive and gram-negative bacterial strains, including MDR isolates (Table 5). The tested gram-positive bacteria included *Staphylococcus aureus* (6538-P) and MRSA (BAA-33591), while the gram-negative bacteria comprised *Escherichia coli* (8739), *Pseudomonas aeruginosa* (9027), the MDR strain *Escherichia coli*

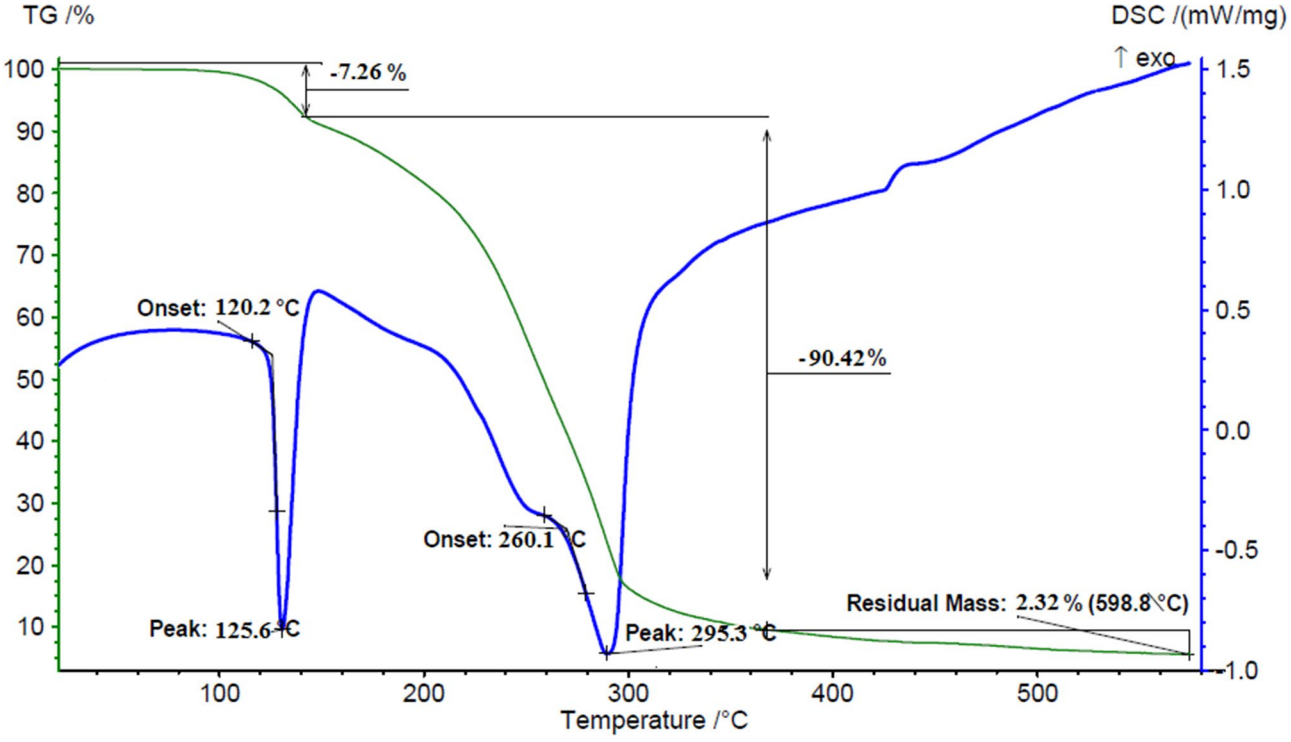

Fig. 6 TGA/DSC analysis curve of the coordination compound [2Ala·HI_3]

Table 4 Thermal analysis of the coordination compound [2Ala·HI_3] by TGA/DSC

S/*N*	Name of the complex	TGA range (^{0}C)	Stage	Mass loss (%)	DSC (^{0}C)	Process	Evolved moiety
1	[2Ala·HI_3].	28–120	I		-	Endo	Dehydration of H_2O
		120–380	II		125.6 295.3	Endo Endo	decomposition of [2Ala·HI_3]

Table 5 Antimicrobial activity of the di-aminopropionic acid hydrogen tri-iodide coordination compound against bacterial strains

Iodine containing compound	**MBC values, µg/ml (I_2 Content Concentration per Total Concentration of the Substance)**						
	EC BAA-2523	**EC 8739**	**SA 33,591**	**SA 6538-P**	**PA 9027**	**PA TA2**	**AB BAA-1790**
[2Ala·HI_3] Coordination Compound	0.49/3.91	0.24/1.95	0.98/7.81	0.49/3.91	0.24/1.95	0.49/3.91	0.98/7.81
Controls	**MBC values, µg/ml (I_2Content Concentration)**						
Lugol's solution	0.56	0.28	1.12	1.12	0.28	0.56	1.12
	MIC values, µg/ml						
Ampicillin sodium salt	500–1000	3.91–7.81	31.25–62.50	3.91–7.81	3.91–7.81	>8000	1000–2000

EC – Escherichia coli; SA – Staphylococcus aureus; PA – Pseudomonas aeruginosa; AB – Acinetobacter baumannii

(BAA-2523), *Acinetobacter baumannii* (ATCC BAA-1790) and the clinical MDR isolate *Pseudomonas aeruginosa* TA2.

The antimicrobial activity was determined by calculating the minimum bactericidal concentration (MBC) for iodine-containing compounds and the minimal inhibitory concentration (MIC) for antibiotics. The synthesised compound demonstrated significant antibacterial activity against all tested gram-positive and gram-negative strains, including MDR bacteria.

According to Morales et al. [30], MIC values are classified as follow: MIC < 100 µg/mL is considered active, 100–500 µg/mL – as moderate, 500–1000 µg/mL – as weak and inactive if the MIC > 1000 µg/mL. Based on these criteria, the di-aminopropionic acid hydrogen tri-iodide compound exhibited high antimicrobial activity, with MBC values ranging between 0.24 µg/mL and 0.98 µg/mL. This reflects superior efficacy compared to the reference compound Lugol's solution and ampicillin sodium.

The best antibacterial effects were observed against *E. coli* 8739 and *P. aeruginosa* 9027, with MBC values of 0.24 µg/mL. Slightly higher MBC values were noted for *E. coli* BAA-2523, *S. aureus* 6538-P and *P. aeruginosa* TA2 (0.49 µg/mL), while *S. aureus* 33,591 and *A. baumannii* BAA-1790 showed MBC values of 0.98 µg/mL.

The [2Ala·HI_3] coordination compound displayed significant bactericidal activity across all tested strains, outperforming Lugol's solution and ampicillin sodium. Importantly, its high efficacy against MDR strains highlights its potential for treating acute and chronic infections caused by resistant bacteria. This study establishes the compound as a promising candidate for further development in antimicrobial therapies.

Conclusion

This study introduced diaminopropionic acid hydrogen triiodide [2Ala·HI3], a novel coordination compound, and demonstrated its potent antimicrobial activity against both susceptible and multidrug-resistant (MDR) bacterial strains. The compound exhibited high inhibitory and bactericidal effects, outperforming standard agents like Lugol's solution and ampicillin sodium in certain cases. These findings suggest that [2Ala·HI_3] has significant potential as a candidate for new antimicrobial drugs, particularly for infections caused by resistant pathogens.

Despite these promising results, the study has certain limitations. The antimicrobial spectrum of the compound was not fully explored due to the limited range of pathogens tested. Expanding this scope to include additional bacterial species and fungi would provide a more comprehensive understanding of its efficacy. Additionally, the potential cytotoxicity of the compound to human cells was not assessed, an essential consideration for evaluating its safety in clinical applications. Finally, the mechanism of action remains unclear, leaving questions about its interaction with bacterial cells and resistance potential unanswered. Further studies addressing these limitations will be crucial for validating the compound's therapeutic potential and advancing it toward clinical development.

Abbreviations

DSC	Differential scanning colorimeter
EDX	Energy-dispersive X-ray spectroscopy
MBC	Iodine-containing compounds
MIC	Minimal inhibitory concentration
MDR	Multidrug resistance
RT	Room temperature
TG	Thermogravimetry

Supplementary Information

The online version contains supplementary material available at https://doi.org/10.1186/s13104-024-07052-8.

Supplementary Material 1

Acknowledgements

The authors would like to thank the control and analytical laboratory of SCAID for assisting in preparing the materials for the article.

Author contributions

S.T., A.I. and A.A developed the idea for the research. S.T., A.K and A.J. performed all the experiments and collected the data. S.K. and D.A. analysed and interpreted the data and were major contributors to the writing of the manuscript. All the authors have read and approved the final manuscript.

Funding
The research was carried out within the framework of the scientific and technical project "Improvement of measures to ensure biological safety in Kazakhstan: Counteraction to dangerous and especially dangerous infections" (IRN BR218004/0223 2023-2025).

Data availability
No datasets were generated or analysed during the current study.

Declarations

Ethics approval and consent to participate
Not applicable.

Consent for publication
Not applicable.

Competing interests
The authors declare no competing interests.

Received: 5 July 2024 / Accepted: 19 December 2024
Published online: 25 December 2024

References

1. Murray CJL, Ikuta KS, Sharara F, Swetschinski L, Aguilar GR, Gray A, Han C, Bisignano C, Rao P, Wool E, Johnson SC, Browne AJ, Chipeta MG, Fell F, Hackett S, Haines-Woodhouse G, Hamadani BHK, Kumaran E, McManigal B, Naghavi M. Global burden of bacterial antimicrobial resistance in 2019: a systematic analysis. Lancet. 2022;399(10325):629–55. https://doi.org/10.1016/s0140-6736(21)02724-0. a. P.
2. Drug-Resistant Infections. A threat to our economic future. (2017). In *World Bank*. https://www.worldbank.org/en/topic/health/publication/drug-resistant-infections-a-threat-to-our-economic-future
3. Kunisada T, Yamada K, Oda S, Hara O. Investigation on the efficacy of povidone-iodine against antiseptic-resistant species. Dermatology. 1997;195(2):14–8. https://doi.org/10.1159/000246025.
4. Yasuda T, Yoshimura Y, Takada H, Kawaguchi S, Ito M, Yamazaki F, Iriyama J, Ishigo S, Asano Y. Comparison of Bactericidal effects of commonly used antiseptics against pathogens causing nosocomial infections. Dermatology. 1997;195(2):19–28. https://doi.org/10.1159/000246026.
5. Lachapelle JM, Castel O, Casado AF, Leroy B, Micali G, Tennstedt D, Lambert J. Antiseptics in the era of bacterial resistance: a focus on povidone iodine. Clin Pract. 2013;10(5):579–92. https://doi.org/10.2217/cpr.13.50.
6. Kawana R, Kitamura T, Nakagomi O, Matsumoto I, Arita M, Yoshihara N, Yanagi K, Yamada A, Morita O, Yoshida Y, Furuya Y, Chiba S. Inactivation of human viruses by povidone-iodine in comparison with other Antiseptics. Dermatology. 1997;195(2):29–35. https://doi.org/10.1159/000246027.
7. Wutzler P, Sauerbrei A, Klöcking R, Bröggmann B, Reimer K. Virucidal activity and cytotoxicity of the liposomal formulation of povidone-iodine. Antiviral Res. 2002b;54(2):89–97. https://doi.org/10.1016/s0166-3542(01)00213-3.
8. Hoekstra MJ, Westgate SJ, Mueller S. Povidone-iodine ointment demonstrates in vitro efficacy against biofilm formation. Int Wound J. 2016b;14(1):172–9. https://doi.org/10.1111/iwj.12578.
9. Oduwole KO, Glynn AA, Molony DC, Murray D, Rowe S, Holland LM, McCormack DJ, O'Gara JP. Anti-biofilm activity of sub-inhibitory povidone-iodine concentrations against Staphylococcus epidermidis and Staphylococcus aureus. J Orthop Research®. 2010b;28(9):1252–6. https://doi.org/10.1002/jor.21110.
10. Johani K, Malone M, Jensen SO, Dickson HG, Gosbell IB, Hu H, Yang Q, Schultz G, Vickery K. Evaluation of short exposure times of antimicrobial wound solutions against microbial biofilms: from in vitro to in vivo. J Antimicrob Chemother. 2017b;73(2):494–502. https://doi.org/10.1093/jac/dkx391.
11. Capriotti P, Barone, Capriotti. Efficacy of dilute povidone-iodine against multidrug resistant bacterial biofilms, fungal biofilms and fungal spores. J Clin Res Dermatology. 2018;5(1):1–5. https://doi.org/10.15226/2378-1726/5/1/00174.
12. Isenberg SJ. The ocular application of povidone-iodine. PubMed. 2003;16(46):30–1. https://pubmed.ncbi.nlm.nih.gov/17491857.
13. Benevento WJ, Murray P, Reed CA, Pepose JS. The sensitivity of Neisseria gonorrhoeae, Chlamydia trachomatis, and herpes simplex type II to Disinfection with Povidone-Iodine. Am J Ophthalmol. 1990;109(3):329–33. https://doi.org/10.1016/s0002-9394(14)74560-x.
14. Lepelletier D, Maillard JY, Pozzetto B, Simon A. Povidone iodine: Properties, mechanisms of action, and role in infection control and staphylococcus aureus decolonization. Antimicrob Agents Chemother. 2020;64(9). https://doi.org/10.1128/aac.00682-20.
15. Beukelman CJ, Van Den Berg AJJ, Hoekstra MJ, Uhl R, Reimer K, Mueller S. Anti-inflammatory properties of a liposomal hydrogel with povidone-iodine (Repithel®) for wound healing in vitro. Burns. 2008;34(6):845–55. https://doi.org/10.1016/j.burns.2007.11.014.
16. Kanagalingam J, Feliciano R, Hah JH, Labib H, Le TA, Lin J. Practical use of povidone-iodine antiseptic in the maintenance of oral health and in the prevention and treatment of common oropharyngeal infections. Int J Clin Pract. 2015;69(11):1247–56. https://doi.org/10.1111/ijcp.12707.
17. Bigliardi PL, Alsagoff SaL, El-Kafrawi HY, Pyon JK, Wa CTC, Villa MA. Povidone iodine in wound healing: a review of current concepts and practices. Int J Surg. 2017;44:260–8. https://doi.org/10.1016/j.ijsu.2017.06.073.
18. Rikimaru T, Kondo M, Kajimura K, Hashimoto K, Oyamada K, Sagawa K, Tanoue S, Oizumi K. Bactericidal activities of commonly used antiseptics against multidrug-resistant mycobacterium tuberculosis. Dermatology. 2002;204 Suppl 1:15–20. https://doi.org/10.1159/000057719. PMID: 12011515.
19. Sun W, Wang ZX, Guo Y, Li C, Gao G, Wu FG. Iodine/soluble starch cryogel: an iodine-based antiseptic with instant water-solubility, improved stability, and potent bactericidal activity. Carbohydr Polym. 2024;340:122217. https://doi.org/10.1016/j.carbpol.2024.122217. Epub 2024 Apr 30. PMID: 38857997.
20. Rikimaru T, Kondo M, Kajimura K, Hashimoto K, Oyamada K, Miyazaki S, Sagawa K, Aizawa H, Oizumi K. Efficacy of common antiseptics against multidrug-resistant Mycobacterium tuberculosis. Int J Tuberc Lung Dis. 2002;6(9):763–70. PMID: 12234131.
21. Ilin AI, Kulmanov ME, Korotetskiy IS, Islamov RA, Akhmetova GK, Lankina MV, Reva ON. Genomic insight into mechanisms of reversion of Antibiotic Resistance in Multidrug Resistant *Mycobacterium tuberculosis* Induced by a Nanomolecular iodine-containing complex FS-1. Front Cell Infect Microbiol. 2017;7:151. https://doi.org/10.3389/fcimb.2017.00151. PMID: 28534009; PMCID: PMC5420568.
22. Reva ON, Korotetskiy IS, Joubert M, Shilov SV, Jumagaziyeva AB, Suldina NA, Ilin AI. The Effect of Iodine-Containing Nano-Micelles, FS-1, on Antibiotic Resistance, Gene expression and epigenetic modifications in the genome of Multidrug resistant MRSA strain *Staphylococcus aureus* ATCC BAA-39. Front Microbiol. 2020;11:581660. https://doi.org/10.3389/fmicb.2020.581660. PMID: 33193215; PMCID: PMC7642360.
23. Kenesheva ST, Taukobong S, Shilov SV, Kuznetsova TV, Jumagaziyeva AB, Karpenyuk TA, Reva ON, Ilin AI. The Effect of three complexes of iodine with amino acids on Gene expression of Model Antibiotic resistant microorganisms Escherichia coli ATCC BAA-196 and Staphylococcus aureus ATCC BAA-39. Microorganisms. 2023;11(7):1705. https://doi.org/10.3390/microorganisms11071705.
24. Methods for Dilution Antimicrobial Susceptibility Tests for Bacteria That Grow Aerobically. Approved standard—Tenth Edition. CLSI document M07-A10. Wayne, PA: Clinical and Laboratory Standards Institute; 2015.
25. Performance Standards for Antimicrobial Susceptibility Testing. CLSI supplement M100. 28th ed. Wayne, PA: Clinical and Laboratory Standards Institute; 2018.
26. Andrews JM. Determination of minimum inhibitory concentrations. J Antimicrob Chemother. 2001;48(suppl1):5–16. https://doi.org/10.1093/jac/48.suppl_1.5.
27. Morsch L, Farmer S, Cunningham K, Sharrett Z, Shea KM. Organic Chemistry II (2023). Open educational resources: Textbooks, Smith College, Northampton, MA. https://scholarworks.smith.edu/textbooks/6
28. Nakamoto K. Infrared Raman Spectra Inorg Coord Compd. 2008. https://doi.org/10.1002/9780470405840.
29. Parikh K, Joshi J, Joshi M. Influence of organic dopants (L-alanine and L-arginine) on structural, spectroscopic and thermal properties of ammonium dihydrogen phosphate crystal. Mater Science-Poland. 2017;35(3):632–8. https://doi.org/10.1515/msp-2017-0067.

30. Morales G, Paredes A, Sierra P, Loyola LA. Antimicrobial activity of three Baccharis species used in the Traditional Medicine of Northern Chile. Molecules. 2008;13(4):790–4. https://doi.org/10.3390/molecules13040790.